CrystEngComm

Accepted Manuscript

ROYAL SOCIETY OF CHEMISTRY

www.rsc.org/crystengcomm

CrystEngComm RSCPublishing

COMMUNICATION

www.rsc.org/

Cite this: DOI: 10.1039/x0xx00000x

Functionalising metal–organic frameworks with metal complexes: the role of structural dynamics

Received ooth June 2015,
Accepted ooth June 2015

DOI: 10.1039/x0xx00000x

Ana E. Platero-Prats,[‡a,b,c,d] Antonio Bermejo Gómez,[‡a,b,e] Karena W. Chapman,[d] Belén Martín-Matute[*a,b] and Xiaodong Zou[*a,c]

A series of iridium-functionalised UiO-67 metal-organic frameworks (MOFs) were synthesised under conditions that simulate kinetically- and thermodynamically-controlled regimes. The degree of functionalisation depends on the reaction time and relative acidity of the native- and metallo-linkers, and can be optimised by controlling the reaction time.

Well-defined metal sites in nanoporous metal-organic frameworks (MOFs) are source of diverse functional behaviours including catalytic activity,[1-4] light-harvesting for solar energy conversion[5] or sorption selectivity.[6,7] Metal ions are integral to the framework itself, connecting the organic linkers at nodes in the framework, with an additional possibility of being coordinated in metallo-linkers or providing charge balance within pores. Exchanging or adding metal ions at target sites can enhance or tune metal-based functionalities. Within the nodes, the metal ions/clusters strongly influence the structure and topology of the resulting framework, thereby limiting the variety of metal ions that are directly incorporated during synthesis. For metallo-linkers, where metal ions can be coordinated to functionalised linkers, a broader range of metal ions may be accommodated. Within such metallo-linkers, not only are the metal sites readily accessible for catalytic reactions, but their properties can also be tuned through variation of the ligands that complete the coordination sphere of the metals. For this reason, understanding metallo-linker functionalisation of MOFs is of both fundamental and applied importance.

‡ These authors equally contributed to this work.
[a] Berzelii Centre EXSELENT on Porous Materials, SE-10691 Stockholm, Sweden. E-mail: xzou@mmk.su.se, belen.martin.matute@su.se
[b] Department of Organic Chemistry, Stockholm University, SE-10691 Stockholm, Sweden.
[c] Department of Materials and Environmental Chemistry, Stockholm University, SE-10691 Stockholm, Sweden.
[d] X-ray Science Division, Advanced Photon Source, Argonne National Laboratory, Argonne, IL 60439, USA.
[e] Current Address: AstraZeneca Translational Science Centre at Karolinska Institute, SE-17165 Stockholm, Sweden.
†Electronic Supplementary Information (ESI) available: synthesis procedures, ^{1}H NMR spectroscopy analyses and XRPD studies. See DOI: 10.1039/c000000x/

Challenges related to materials synthesis and characterisation have limited the degree of metal functionalisation that can be achieved in MOFs. Metallo-linkers can be included in MOFs directly, during the synthesis of the framework itself, or post-synthetically. The former[8,9] can allow direct synthesis of the target composition, even without first isolating the metallo-linker.[10] Post-synthetic approaches, including metallations of potential metallo-linkers,[2,3,6,11,12] for example, those based on 2,2′-bipyridyl moieties, require initial synthesis of the pristine MOF, followed by a separate metallation reaction. Recently, post-synthetic modification has been achieved by exchange of linkers, metallo-linkers, or metals upon immersion of the MOF in solution.[13-15] This approach exploits the porosity and dynamic nature of MOF structures.[16]

Metallo-functionalisation in these dynamic systems can lead to structural and chemical heterogeneity, competing side reactions, metal liability and loss, and framework destabilisation, all of which present a characterisation challenge. Careful compositional and structural analyses must be combined to develop an understanding of metal functionalisation and the associated mechanism from kinetic and thermodynamic viewpoints. Controlling kinetic and thermodynamic effects is key to achieving highly-functionalised systems with homogeneously-distributed metal-sites.

The high thermal and chemical stability of zirconium-based MOFs makes them ideal model systems for exploring metal-based functionalisation of MOFs. The Zr-MOF UiO-67[17-19] (**fcu** topology, *F23*, a = 27.094 Å), based on a biphenyl linker, has been a recent focus of such efforts. Its structure is formed by linear bridging of 8-connected $[Zr_6O_4(OH)_4]$ nodes by 1,1′-biphenyl-4,4′-dicarboxylate linkers (bpdc), resulting in composition $[Zr_6O_4(OH)_4(bpdc)_6]$ for the standard MOF. The open framework defines edge-sharing octahedral cages (Figure 1a). The bpdc linker in UiO-67 can be replaced by either metallated or unmetallated 2,2′-bipyridyl-5,5′-dicarboxylate (bpydc) linker (Figure 1b). These analogues have composition $[Zr_6O_4(OH)_4(bpdc)_{6-y}(X)_y]$, where X is either the metallo-linker and/or the unmetallated bpydc linker. Each octahedral cage has 12 edges, 2y of them are metallo-linkers, shared with neighbouring octahedral cages (Figure 1c).

Here we explore the impact of kinetic and thermodynamic reaction conditions on the composition, structure, and crystallinity of

UiO-67 functionalised with the iridium complex [Cp*Ir(bpydc)(Cl)Cl]$^{2-}$ (denoted as Ir-**L**, Cp* = pentamethylcyclopentadienyl). Iridium-complexes have been incorporated in UiO-67 for catalytic and light harvesting applications.[8,12]

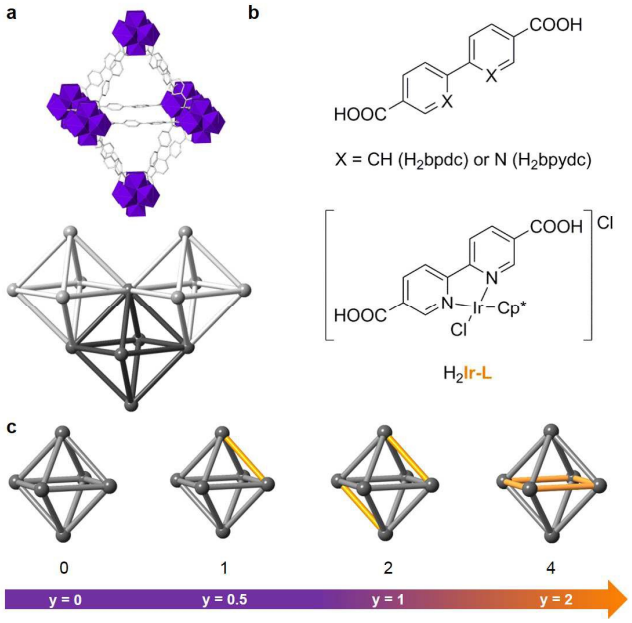

Figure 1 a) The octahedral cage in UiO-67 and its connection to the neighbouring cages. b) H_2bpdc and H_2bpydc linkers, and iridium metallo-linker used here. c) Representation of degrees of functionalisation, $[Zr_6O_4(OH)_4(bpdc)_{6-y}(X)_y]$.

Ir-**L** substituted UiO-67 samples were prepared directly from mixtures of H_2bpdc and H_2Ir-**L** under hydrothermal reaction conditions at 100 °C. Three different H_2bpdc / H_2Ir-**L** ratios, 1:12, 2:12, and 4:12 (corresponding to y = 0.5, 1 and 2, respectively), were used, each with two different reaction times, 12 and 36 h. The samples are denoted based on their y values as **0.5**, **1** and **2** for 12 h reaction time and **0.5′**, **1′** and **2′** for 36 h reaction time. Similar yields (*ca.* 65% for 12 h and 70-85% for 36 h) were obtained under all conditions and for all H_2bpdc / H_2Ir-**L** ratios used. H_2Ir-**L** was synthesised from $[Cp^*IrCl_2]_2$ and H_2bpydc,[14] and used either directly as the crude reaction mixture (Method B) or as the isolated metallo-linkers (Method A) in the UiO-67 synthesis (Section S1, †ESI). The linker composition (bpdc : Ir-**L** : bpydc) in each Ir-UiO-67 product was evaluated by ^{1}H Nuclear Magnetic Resonance (NMR) spectroscopy after digestion of the samples under mild acidic conditions.[10] Both synthetic methods yielded Ir-UiO-67 with similar composition (Table S1, †ESI). Structural analyses of the MOFs were undertaken based on transmission X-ray powder diffraction (XRPD) data obtained from a Panalytical X'Pert PRO diffractometer equipped with CuKα radiation. Only results for Method B are presented here. The results for Method A are included in the supporting information (Section S2 and S3, †ESI).

As shown in Table 1 and Table S1 (†ESI), the isolated Ir-UiO-67 samples contained bpdc, Ir-**L**, and Ir-free bpydc, indicating that partial demetallation of the linker occurred during the synthesis. While the Ir-**L** content in the Ir-UiO-67 sample increased with the Ir concentration in the initial synthesis mixture, it decreased with prolonged reaction time. The highest functionalisation with iridium was obtained for sample **2** after 12 h reaction time (Table 1, entry 3). The Ir demetallation (Ir-**L** → bpydc) also increased with prolonged reaction time, from 21-25% at 12 h (Table 1, entries 1-3 and Table S1, entries 1-3) to 41-56% at 36 h (Table 1, entries 4-6 and Table S1, entries 4-6). After 12 h, the Ir-**L** / bpdc ratio in the UiO-67 product was higher than that used in the initial synthetic mixture (see Figure 2). After 36 h, the Ir-**L** / bpdc ratio in the UiO-67 product decreased and became lower than that in the initial synthetic mixture. Our earlier thermal gravimetric analyses and infrared spectroscopy studies of UiO-67 synthesised under these hydrothermal conditions showed there is no evidence for linker vacancies or un-coordinated Ir-**L** metallo-ligand within the pores.[10] This indicates that Ir-**L** metallo-linkers in the MOF were replaced by bpdc linkers with prolonged reaction time.

Table 1. Ir-**L** content, total functionlisation, and Ir demetallation, as determined by ^{1}H NMR spectroscopy for digested Ir-UiO-67 samples.

Entry	Sample	t (h)	No. of Ir-**L** per 6 linkers (y_{UiO})	Total functionalisation (%) [a]	Ir demetallation (%) [b]
1	**0.5**	12	0.58	12	21
2	**1**	12	1.18	26	25
3	**2**	12	2.38	53	25
4	**0.5′**	36	0.23	7	48
5	**1′**	36	0.31	12	56
6	**2′**	36	0.91	26	41

[a] (Ir-**L** + bpydc) / (Ir-**L** + bpydc + bpdc). [b] (bpydc) / (Ir-**L** + bpydc).

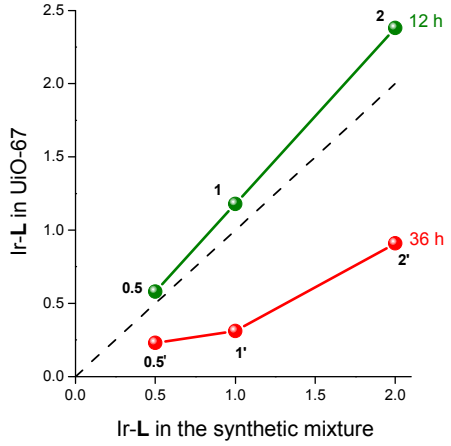

Figure 2 Ir-**L** functionalisation (y_{UiO}, number of Ir-**L** per 6 linkers) in UiO-67 prepared using Method B, derived from digested Ir-UiO-67 samples, relative to the number of Ir-**L** per 6 linkers (y_{soln}) in the synthetic mixture. Those with reaction time 12 and 36 h are shown in green and red, respectively. The dash line corresponds to $y_{UiO} = y_{soln}$.

XRPD showed that the Ir-UiO-67 samples have varying crystallinities, i.e., different degrees of long range structural ordering (Figure 3). Samples with lower degrees of linker incorporation afforded more ordered framework structures. The one with the poorest crystallinity was that with the highest Ir content (sample **2**, y_{UiO} = 2.38), obtained at 12 h. The crystallinity of this reaction product increased significantly after 36 h, with the loss of the iridium metal (sample **2′**, y_{UiO} = 0.91). Investigation of structural models, where bpdc is replaced by Ir-**L**, indicates that due to steric hindrance, maximum one metallo-linker can be installed at each face of the octahedral cage (Figure 4a). There are eight faces per cage; each face is shared by two octahedra. This suggests that the maximum functionalisation is four Ir-**L** metallo-linkers per octahedral cage, i.e., y_{UiO} = 2. This may

contribute to the low crystallinity of **2**, whose functionalisation is slightly above to this limit such that strain and distortions of the lattice occur.

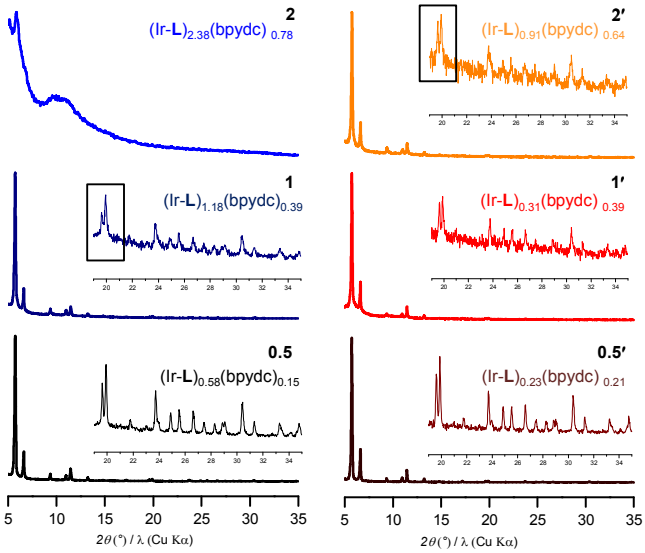

Figure 3 XRPD patterns collected on Ir-UiO-67 samples synthesised following Method B (left, 12 h; right, 36 h), evidencing differences in the relative peak intensity of Bragg reflections at high 2θ range.

There are variations in the relative intensities of certain reflections in the diffraction data, which depend on the synthetic conditions. This can be seen, for example in the (531) and (600) peaks at 2-theta of ~20° (Figure 3, Figure S1 and S2, †ESI). Rietveld refinements were performed on the XRPD data of each sample using two different functionalisation models, with space group *F*23 (cubic) and *F*222 (orthorhombic), respectively (Figure 4b, Figure S3-12, Table S2, †ESI). In the cubic model, the Ir-**L** linkers are randomly distributed over the 12 edges of octahedral cage (*F*23, Figure 4b), while in the orthorhombic model, the Ir-**L** linkers are distributed over four perpendicular edges of octahedral cage (*F*222, Figure 4b), avoiding occupying adjacent edges separated by <90°. Rietveld refinements show that with high degrees of Ir-**L** functionalisation (y > 0.9), the orthorhombic models give better fits to the experimental XRPD patterns than the cubic models do (Figure 4c, Figure S5, S8 and S12, Table S2, †ESI). Furthermore, the structure turns to be more orthorhombic with prolonged reaction time (from 12h to 36 h) (Figure 4d and 4e, Figure S3-12, Table S2, †ESI). This suggests that as the reaction proceeds, the Ir distribution refines to avoid steric conflicts.

The present results indicate that incorporation of Ir-**L** metallo-linkers within UiO-67 depends on the reaction time. Samples isolated after 12 h were enriched in Ir-**L** compared to the reaction mixture (i.e. the ratio Ir-**L** / bpdc was higher in the MOF than the initial ratio used for its synthesis). This can be rationalised based on the higher acidity of H_2Ir-**L** relative to that of H_2bpdc, which contributes to a faster deprotonation of H_2Ir-**L** and results in a higher concentration of Ir-**L** for coordination to Zr. Ir-UiO-67 obtained under these conditions had a non-preferential distribution of Ir on the edges of octahedral cages. The reduced crystallinity in the sample with the highest Ir concentration may result from steric effects of Ir-**L** located on proximal edges wherein local strain and lattice distortions occur.

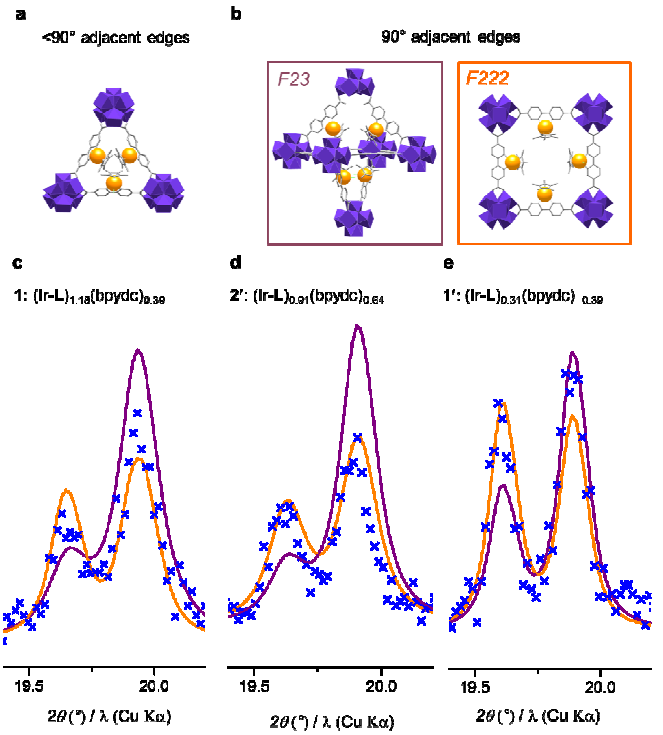

Figure 4 a-b) Representation of different functionalisation in UiO-67. a) Maximum one Ir-**L** linker can occupy each triangular face of the octahedral cage due to steric hindrance. b) Models corresponding to cubic (*F*23) and orthorhombic (*F*222) symmetry. Ir atoms are marked as orange balls. c-e) XRPD patterns simulated from the cubic (purple line) and orthorhombic (orange line) models compared with the experimental XRPD pattern (crosses) for samples **1** (c), **2'** (d) and **1'** (e) in the region containing (531) and (600) peaks.

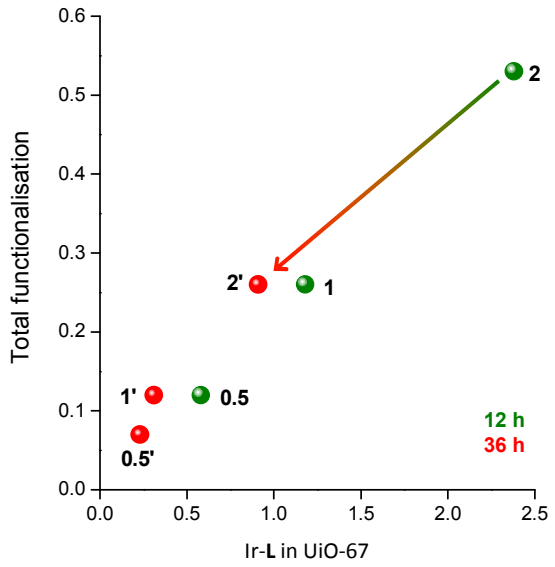

Figure 5 Total functionalisation vs. Ir-**L** content in Ir-UiO-67 samples for 12 h and 36 h. The arrows indicate the loss of functionalisation from 12 to 36 h of reaction time for each reaction mixture.

The changes in MOF composition and crystallinity for identical synthetic mixtures at longer reaction time reflect a more thermodynamically stable state of the system (Figure 5 according to

Table 1). With a progressive loss of Ir (i.e. demetallation), and exchange of Ir-**L** and bpydc linkers by bpdc linkers at the preferred edges with time, it is clear that the Ir-functionalised MOF is metastable with respect to standard UiO-67. The higher energy of the Ir-containing system can be understood from increased strain and reduced crystallinity associated with unfavourable steric interactions of proximal Ir complexes. This effect has likely limited the levels of metallo-functionalisation that have been achieved to date in MOFs. Allowing reactions to continue for longer times will yield more stable structures with lower Ir-loadings, upon demetallation, and with an optimal distribution of the remaining Ir centres to minimise steric interactions.

Conclusions

We have shown that functionalisation of UiO–67 with the iridium complex $[Cp^*Ir(bpydc)(Cl)Cl]^{2-}$ is first controlled kinetically as a result of the acidity of the linkers and metallo-linkers in the reaction mixture. Upon prolonged reaction times, the MOF evolves towards a more thermodynamically stable form, which is achieved through demetallation and linker exchange in solution. An impressive total functionlisation of more than 50% could be obtained in UiO–67 after a reaction time of only 12 h. A prolonged reaction time (36 h) resulted in demetallation. In addition, with time, the metallo-linkers (Ir-**L**) and those resulting from demetallation (bpydc) were exchanged by non-functionalised linkers (bpdc) yielding low functionalised MOFs. Therefore, by optimising the reaction times and controlling the relative acidity of the linkers and metallo-linkers, it is possible to achieve high degree of metallo-functionalisation in MOFs.

Acknowledgements

This project was supported by the Knut and Alice Wallenberg Foundation, the Swedish Research Council (VR), the Swedish Governmental Agency for Innovation Systems (VINNOVA) through the Berzelii Centre EXSELENT on Porous Materials, and the U.S. Department of Energy, Office of Science, Office of Basic Energy Sciences, under Contract No. DE-AC02-06CH11357. B.M.-M. also thanks VINNOVA for a VINNMER grant. A.E.P.-P. was supported by MATsynCELL project through Röntgen–Ångström Cluster, and a Beatriu de Pinós fellowship (BP-DGR 2014) from the Ministry of Economy and Knowledge (Catalan Government).

Notes and references

1. L. Ma, J. M. Falkowski, C. Abney and W. Lin, *Nat. Chem.*, 2010, **2**, 838.
2. F. Carson, S. Agrawal, M. Gustafsson, A. Bartoszewicz, F. Moraga, X. Zou and B. Martín-Matute, *Chem. Eur. J.*, 2012, **18**, 15337.
3. J. Juan-Alcañiz, J. Ferrando-Soria, I. Luz, P. Serra-Crespo, E. Skupien, V. P. Santos, E. Pardo, F. X. Llabrés i Xamena, F. Kapteijn and J. Gascon, *J. Catal.*, 2013, **307**, 295.
4. P. V. Dau and S. M. Cohen, *Chem. Commun.*, 2013, **49**, 6128.
5. H.-J. Son, S. Jin, S. Patwardhan, S. J. Wezenberg, N. C. Jeong, M. So, C. E. Wilmer, A. Sarjeant, G. C. Schatz, R. Q. Snurr, O. K. Farha, G. P. Wiederrecht and J. T. Hupp, *J. Am. Chem. Soc.*, 2013, **135**, 862.
6. E. D. Bloch, D. Britt, C. Lee, C. J. Doonan, F. J. Uribe-Romo, H. Furukawa, J. R. Long and O. M. Yaghi, *J. Am. Chem. Soc.*, 2010, **132**, 14382.
7. G. Nickerl, M. Leistner, S. Helten, V. Bon, I. Senkovska and S. Kaskel, *Inorg. Chem. Front.*, 2014, **1**, 325.
8. C. Wang, Z. Xie, K. E. de Krafft and W. Lin, *J. Am. Chem. Soc.*, 2011, **133**, 13445.
9. C. Wang, J.-L. Wang and W. Lin, *J. Am. Chem. Soc.*, 2012, **134**, 19895.
10. A. E. Platero-Prats, A. Bermejo Gómez, L. Samain, X. Zou and B. Martín-Matute, *B. Chem. Eur. J.*, 2015, **21**, 861.
11. A. M. Rasero-Almansa, A. Corma, M. Iglesias and F. Sánchez, *Green Chem.*, 2014, **16**, 3522.
12. K. Manna, T. Zhang, W. Lin, *J. Am. Chem. Soc.*, 2014, **136**, 6566.
13. P. Deria, W. Bury, J. T. Hupp and O. K. Farha, *Chem. Commun.*, 2014, **50**, 1965.
14. S. Pullen, H. Fei, A. Orthaber and S. M. Cohen, S. Ott, *J. Am. Chem. Soc.*, 2013, **135**, 16997.
15. F. Carson, E. Martínez-Castro, R. Marcos, G. González Miera, K. Jansson, X. Zou, B. Martín-Matute, *Chem. Commun.*, 2015, **51**, 10864.
16. C. Serre, C. Mellot-Draznieks, S. Surblé, N. Audebrand, Y. Filinchuk and G. Ferey, *Science*, 2005, **315**, 1828.
17. H. Cavka, S. Jakobsen, U. Olsbye, N. Guillou, C. Lamberti, S. Bordiga and K. P. Lillerud, *J. Am. Chem. Soc.*, 2008, **130**, 13850.
18. M. I. Gonzalez, E. D. Bloch, J. A. Mason, S.J. Teat and J. R. Long, *Inorg. Chem.*, 2015, **54**, 2995.
19. X. Yu and S. M. Cohen, *Chem. Commun.*, 2015, **51**, 9880.

Table of Contents

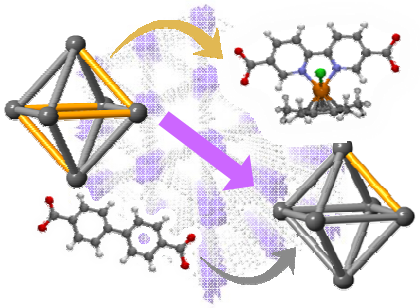

The impact of dynamics in the functionalisation of metal-organic framework UiO-67 with an Ir-complex has been studied. Highly functionalised Ir-UiO-67 can be only trapped as kinetic products, which lose metals and exchange species to gain stability.